A R C H I V E O F M E C H A N I C A L E N G I N E E R I N G

VOL. LXV 2018 Number 2

DOI: 10.24425/123024

Key words: 3-D computer multibody simulation (MBS) model, braking time, friction forces, normal forces, radial run-out, impact function based contact

YANKO SLAVCHEV [1], *LUBOMIR DIMITROV* [2], *YAVOR DIMITROV* [2]

3-D COMPUTER RESEARCH AND COMPARATIVE ANALYSIS OF DYNAMIC ASPECTS OF DRUM BRAKES AND CALIPER DISC BRAKES

This paper presents the construction of adequate 3-D computer models for simulation research and analysis of dynamic aspects of caliper disc brakes, as well as of drum brakes, actuated by a short stroke electromagnet or a hydraulic thruster, when these brake types are used in the hoisting mechanism of cranes. The adequacy of the 3-D models has been confirmed by comparing their simulation results with results from an experiment and from classic computational models.

The classic computational models, related to the study of main dynamic features of friction brakes, are layouts that are based on a number of assumptions, such as that the braking force instantly reaches its steady-state value, the clearance between the friction lining and the disc/drum is neglected, etc. These assumptions lead to a limitation of research options.

The proposed 3-D computer models improve the research layouts by eliminating a number of the classic model assumptions. The improvements are related to the determination of the braking time, braking torque, normal force and other dynamic aspects of the brakes by performing simulations that take into account: the braking force as a function of time, the presence of clearance between the friction lining and the disc/drum, etc.

Nomenclature

$D_d = 2R_d$ drum diameter, m

$\mathrm{d}p/\mathrm{d}t$ penetration velocity at the point of contact, m/s

[1] *Technical University – Sofia, Faculty of Mechanical Engineering, Kl. Ohridsky 8 blvd., 1000, Sofia, Bulgaria. Email: ya_slavchev@abv.bg*

[2] *Mechanical Engineering Department, Technical University – Sofia, Faculty of Mechanical Engineering, Kl. Ohridsky 8 blvd., 1000, Sofia, Bulgaria. Emails: lubomir_dimitrov@tu-sofia.bg, yavor.dimitrov90@gmail.com*

f deformation of the spring element, m

F_s force (spring force) that loads the simulation element (spring element), N

J_1 reduced mass moment of inertia of a crane hoisting system, equipped with drum brake (used also for the brake, experimentally tested in [1]), kgm^2

J_{1u} reduced mass moment of inertia of a crane hoisting system, equipped with drum brake, as calculated in [2], kgm^2

J_2 reduced mass moment of inertia of a crane hoisting system equipped with caliper disc brake (used also for the system in [1] but equipped with SIME 45K type brake), kgm^2

J_{2u} reduced mass moment of inertia of the system in [2] but equipped with SIME 45K type brake, kgm^2

J_{disc} moment of inertia (mass moment of inertia) of the disc, kgm^2

J_{drum} moment of inertia (mass moment of inertia) of the drum, kgm^2

K_d dynamic coefficient

k_f coefficient that accounts for the pad shape, [1]

k_s stiffness of the simulation element (spring element), N/m

p contact penetration, m

Q nominal load capacity, ton

R_{ave} average friction radius, m

R_d drum radius, m

R_e average equivalent friction radius, m

R_i inner friction radius, m

R_o outer friction radius, m

t_B braking time, s

T_B braking torque, Nm

t_{Bu1} braking time for full stop (during load lifting), calculated in [2] for a crane hosting mechanism, equipped with drum brake type TKT-300, s

t_{Bu2} braking time for full stop (during load descent), calculated in [2] for a crane hosting mechanism, equipped with drum brake type TKT-300, s

T_i total inertia torque due to the inertia forces of the rotating and reciprocating bodies, Nm

T_R total reaction torque, Nm

u_M total gear ratio of the hoisting mechanism

Greek symbols

β coefficient that accounts for the efficiency of the mechanism

η_M efficiency coefficient

λ gap between the friction lining and the disc or the drum, mm

μ coefficient of friction

ω nominal angular velocity of the rotating brake element, s^{-1}

1. Introduction

By the beginning of the 90s of the XX century, the drum brakes (external linearly acting, centrally pivoted shoe brakes) were the predominant brakes that were used in a wide range of industrial machinery, including material handling machines [3].

Gradually, beginning from the automotive industry, the introduction of the simplified but effective disc brakes (caliper disc brakes) marked the beginning of the shifting from drum to disc brakes. There started a process of retrofitting with caliper disc brakes of transport vehicles, such as light and heavy trucks, railway vehicles, etc., as well as of machinery for industrial applications, such as cranes, forklifts, conveyors, mining equipment, etc.

Replacing a drum brake with a disc brake may not always result in better dynamic, thermal or other indicators, especially when one takes into account the number of factors for different modes of operation and assembly [4].

In this respect, comparative research and evaluation of the same parameters of drum and disc brakes are necessary. Among the most important parameters are the braking torque, the braking time, the heat generated during the braking process, the frequency and duration of the braking cycles [5]. The differences in the use of diverse types of brakes come down to the importance with which one focuses on certain parameters.

Studies of friction brakes have been carried out for almost a century, mainly by classical mathematical formulations and experiments on specimen or field tests on a stand.

The classical formulations, related to the study of the main dynamic aspects of brakes, are based primarily on rotational computation models and a number of assumptions, such as:

- the braking force reaches instantly its steady-state value;
- the clearance (gap) between the friction lining and the disc/drum is neglected;
- there are no abnormalities in the kinematic chain – the disc/drum have no deviations from roundness and no run-out (radial or lateral).

In the field studies, which are perceived as most credible, it is not always possible to take into account some specifics of the design and the response of the brake during operation.

In addition, these studies are labor-intensive, costly, and provide information about the brake performance after the brake has been manufactured.

In the last two decades, the possibility of more extensive research on dynamic performance of braking systems has been enhanced through computer models and simulations, based on modern CAE tools, such as the finite element method (FEM), multibody dynamics (MBD), etc. For example, references [6–13] have studied in detail the performance of automobile disc and drum brakes and, by the use of the FEM, have analyzed various problems, such as: thermomechanical behavior of the dry contact between the brake disc and pads during the braking phase, influence

of Young's modulus on squeal generation, thermal effects in the structure and the contact behavior of a disc-pad assembly, estimation of heat transfer coefficients (h) of the full and ventilated brake discs as a function of time, etc. Reference [14] has studied the rigid-flexible couple of drum brake system by the use of MBD models.

The use of the modern CAE tools enables the detection of new aspects of brakes performance and application under combined loading conditions, such as in bicycles [15, 16] and also enables optimization of brake system components [17].

In this regard, the main objective of the current paper is the construction of 3-D multibody simulation (MBS) models, which will be used to study and analyze aspects of the dynamic response of friction braking systems.

Through the simulation models, that have been developed, a number of novelties in research capabilities are achieved. Some of the novelties are:

- Consideration of the gap between the friction material and the disc/drum. This is achieved by the use of Hinge mates, located at the points of rotation of the brake elements that carry the pads.
- Consideration of the kinematic chain deviations during assembly. This is achieved by constructing a Hinge mate in the drum/disk hub.
- Controlling the increase of the force in the operating spring. This is achieved by means of balancing force functions, designed in such a way so as to allow for simulations to be carried out on the actuation of different brake designs.
- Attaining increased efficiency in calculating impacts, as compared to known approaches such as FEM. This is due to the adopted MBD approach to modeling, along with its impact-function-based contact algorithm capability and corresponding stiff integration methods for computing motion.

2. Theoretical considerations

2.1. General calculations

During braking, the kinetic energy of the rotating and reciprocating moving parts is converted, through a braking device, into heat energy that is dissipated into the environment.

Motion deceleration is due to the work done mainly by the braking device, but is also due to the reaction forces, both in the mechanism and in the operating part of the machine.

The equation of motion during the braking period is given by the classical relationship:

$$T_B \pm T_R = T_i \,. \tag{1}$$

For hoisting mechanisms, the sign (+) corresponds to braking during load lift, and the sign (−) to braking during load descent.

For most mechanisms, it is assumed, with sufficient accuracy for practical use, that T_R is constant throughout the braking interval [1].

For automatic brakes, that operate under such conditions that the heating of the friction material does not lead to abrupt changes in its friction properties, the braking torque T_B increases very rapidly at first and then settles to a practically constant value within the braking period, Fig. 1.

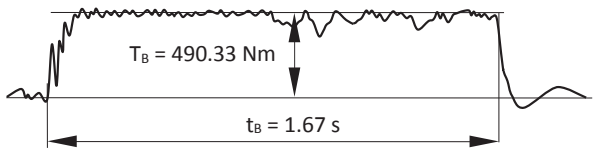

Fig. 1. Change of the braking torque T_B in the braking process [1]

Since T_R and T_B are constant, it follows that T_i is constant too, and

$$T_i = J\varepsilon = \frac{J\omega}{t_B}, \tag{2}$$

where J is the total mass moment of inertia of all rotating and reciprocating bodies, expressed relative to the revolutions of the motor shaft, ω is the angular velocity of the motor shaft.

After substitution in (1) and rework, the well-known relation for the braking time is obtained:

$$t_B = \frac{J\omega}{T_B \pm T_R}. \tag{3}$$

The braking torque T_{B1} of drum brakes is calculated according to the relation [1, 2, 18]

$$T_{B1} = \mu_1 N_1 D_d, \tag{4}$$

where μ_1 is the friction coefficient, N_1 – the normal force acting at the shoe-drum contact.

For caliper disc brakes, the braking torque T_{B2} is calculated according to the relation [1]:

$$T_{B2} = z\mu_2 N_2 R_e, \tag{5}$$

where z is the number of friction pairs (pads–disc), N_2 is the normal axial force at the friction pair,

$$R_e = R_{ave} k_f. \tag{6}$$

The average friction radius R_{ave} could be determined as follows [18]:

- for uniform wear (if pv = const, i.e., if we have a constant product of the pressure p that acts on a given point of the friction surface and the velocity v at this point)

$$R_{ave} = \frac{R_o + R_i}{2}, \tag{7}$$

- for uniform pressure (if it is assumed that the pressure distribution over the entire friction surface is uniform, $pv = \text{const}$ – for new brakes)

$$R_{ave} = \frac{1}{3}\frac{R_o^3 + R_i^3}{R_o^2 - R_i^2}. \tag{8}$$

Computing R_{ave} by any of the two formulas leads to quite similar results [1, 18]. The radii R_o, R_i and R_d are shown in Fig. 2.

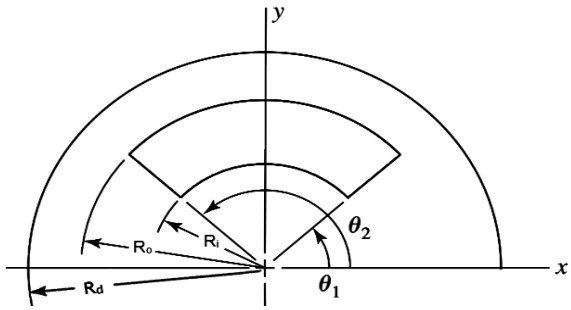

Fig. 2. Contact area scheme of caliper disc brakes with annular pads [18]

2.2. Comparative calculations

Calculations and comparisons are performed for the braking times t_{B1} and t_{B2}, and for the normal forces N_1 and N_2 of drum and caliper disc brake.

From Eq. (1) it follows

$$t_{B1} = \frac{J_1\omega_1}{T_{B1} \pm T_{R1}}, \qquad t_{B2} = \frac{J_2\omega_2}{T_{B2} \pm T_{R2}}. \tag{9}$$

Assuming that $\omega_1 = \omega_2 = \omega$, $T_{B1} = T_{B2} = T_B$, $T_{R1} = T_{R2}$, one obtains

$$t_{B2} = t_{B1}\frac{J_2}{J_1}. \tag{10}$$

Since both of the compared brakes are elements of one and the same chain of forces, then the reduced mass moments of inertia J_1 and J_2 will differ only by the difference of the mass moments of the drum J_{drum} and the disc J_{disc}

$$J_1 - J_2 = \Delta J = J_{drum} - J_{disc}. \tag{11}$$

After substitution in Eq. (10) and transformations, it follows

$$t_{B2} = t_{B1}\left(1 - \frac{J_{drum} - J_{disc}}{J_1}\right). \tag{12}$$

For one and the same braking torques of drum and disc brakes, it has been found that the mass moment of inertia of the drum brakes J_{drum} is greater than the mass moment of inertia of the disc brakes J_{disc}, i.e. $\Delta J > 0$ and from here it follows, according to Eq. (12), that the braking time of disc brakes is less than that of drum brakes.

On the assumption that $T_{B1} = T_{B2}$, $\mu_1 = \mu_2$ and $z = 2$ the normal force N_2 of disc brakes could be expressed as

$$N_2 = N_1 \frac{R_d}{R_e} . \tag{13}$$

Since $R_d > R_e$, it follows that $N_2 > N_1$ i.e. the normal force of caliper disc brakes is greater than the normal force of drum brakes.

3. Constructing 3-D MBS models

3.1. Overview

Multibody simulations (MBS) [19] are popular type of numerical simulations, in which multibody systems (MBSys) consist of various non-deformable (rigid) or elastic bodies. The connections between the bodies are modeled either by kinematic constraints, that limit respective degrees of freedom, or by force elements, such as springs. The popularity of this kind of simulations, for performing dynamic studies and identify relevant laws of motion, has established MBS as an important engineering tool in pre-engineering calculations.

When using MBS, the research process goes through a number of stages, such as building geometry, setting constraints, forces and moments, configuring the solver and outputting results.

3.2. CAD modeling

For the present study, the CAD system SolidWorks is used to build the geometry of the studied brakes, according to relevant design documentation.

The geometry of the following brake types has been constructed: drum brake type TKT-300 with short stroke electromagnet, drum brake type TKTG-300M with hydraulic thruster and caliper disc brake type 45K. Both TKT-300 and TKTG-300M are produced by the Russian company "Parametr" [20] and the caliper disc brake type 45K is produced by the French company SIME [21].

These brakes are actuated automatically. In the event of power (alternating current) failure, the brake is engaged under the action of spring force, and vice versa – when the power is switched on, the spring force is overcame by triggering the action of a short-stroke electromagnet, or a hydraulic device and the brake opens (it is disengaged).

The following figures (Figs 3, 4) show the constructed 3-D CAD models of the studied brakes.

The TKTG-300M brake has similar braking parameters as the brake TKT-300, but differs only in the way of triggering – by a hydraulic thruster that is attached to the base of the brake or to one of the brake levers.

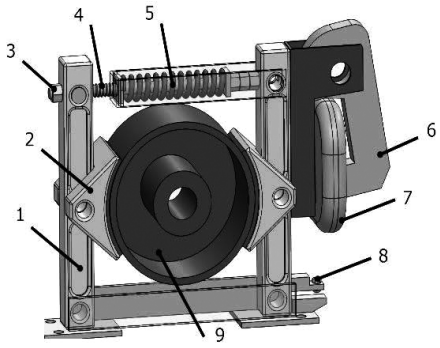

Fig. 3. CAD model of drum brake type TKT-300: 1 – lever, 2 – centrally pivoted external shoe, 3 – rod with nuts for adjusting the braking torque, 4 – auxiliary spring, 5 – operating spring, 6 – armature, 7 – coil, 8 – screw for gap regulation, 9 – brake drum (not a brake element)

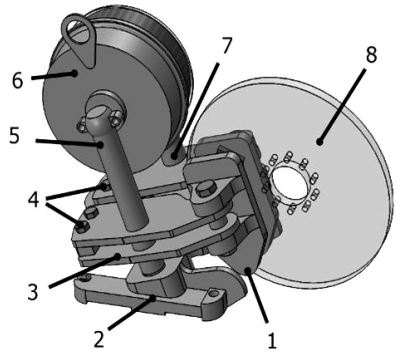

Fig. 4. CAD model of caliper disc brake type SIME 45K: 1 – pad, 2 – base, 3 – lever of a lever-cam mechanism, 4 – bolts for gap regulation, 5 – moving pillar, 6 – electro-magnet, 7 – fixed pillar, 8 – brake disc (not a brake element)

Geometric primitives are used to model the drum/disc, making it possible for the drum/disc shape to be set as not ideally round or not perfectly flat. This allows us to account for deviations in the kinematic chain, such as deviations from roundness, run-out (radial or lateral).

Table 1 lists characteristics of the studied brakes, TKT-300 and SIME 45K.

Once the geometry has been built, the MBS modeling stage begins.

3.3. MBS modeling

This is the most complex stage of the multibody simulation process. Here, boundary conditions, forces, moments, degrees of freedom, etc., are used as inputs so as to convert the multibody system from a 3-D CAD model to a 3-D MBS model, capable of performing motion that corresponds to the movement of the real construction.

SolidWorks Motion is used for the MBS modeling and simulations, due to several reasons.

On the one hand, it is the fact that this product is an add-in module to the SolidWorks CAD system, which makes it possible, when making changes to the CAD model, to transfer quickly these changes to the MBS model.

Table 1.

Brake parameters

No.	Parameter	Brake type	
		TKT-300	45K
1.	Diameter* [mm]	300	315
2.	Thickness* [mm]	140	15
3.	Mass moment of inertia* [kg·m^2]	0.378	0.12
4.	Mass* [kg]	30.283	13.9
5.	Braking torque [Nm] (Duty cycle 25%, 40%)	490.33	410**
6.	Wrap angle [°]	70	60***
7.	Contact area [cm^2]	256.56	56.55
8.	Pad pressure [kgf/cm^2]	1.555	7.797
9.	Friction material	Rolled strip	
10.	Total mass [kg]	92	41

* drum/disc; ** adjustable from −30% to +20%; *** $(\theta_2 - \theta_1)$, Fig. 2

On the other hand, is the fact that this product uses the simulation engine of ADAMS/Solver, which is a module of one of the world-known products for multibody simulations MSC.ADAMS. The simulation engine calculates: displacements, velocities, accelerations, forces, moments, etc., acting on each element of the model.

When building the MBS model, the first step involves assigning appropriate joints between the CAD model elements.

MBS modeling of brake type TKT-300

After all joints are set, a check is made to calculate the model's degrees of freedom (DOF). The results that SolidWorks Motion calculates are summarized in Table 2.

Table 2.

Degrees of freedom of the MBS model of TKT-300

Description	Count	DOF
Moving parts	7	42
Revolute joints	3	15
Fixed joints	2	12
Parallel primitives	2	4
Redundant constraints		0
Total DOF (estimated) (Gruebler count DOF)		11
Total (actual) DOF		11

The moving parts, according to the designations in Fig. 3, are: the two levers, labeled as 1, the two external shoes, labeled as 2 and the friction material fastened to each shoe, the drum, labeled as 9.

The total number of revolute joints is 5 and these joints allow the rotation of the following: the drum, each shoe about the point of its attachment to the respective lever, each lever about the point of its attachment to the support structure. Flexible bushings (which will be explained below in the text) are added to the revolute joints of the shoes, which automatically results in the fact that only 3 of the revolute joints limit the model's degrees of freedom.

The parallel primitives, Fig. 5, are defined for each shoe by a pair of planes, Plane01 and Plane02. The plane Plane01 passes through axis 1 and is a plane of symmetry of the brake shoe. The plane Plane02 is defined by the rotation axes 3 and 4 of the levers. The introduction of the two parallel primitives in the model greatly aids solving the model, as it does not require the use of additional contact conditions and fasteners that are involved in the actual construction.

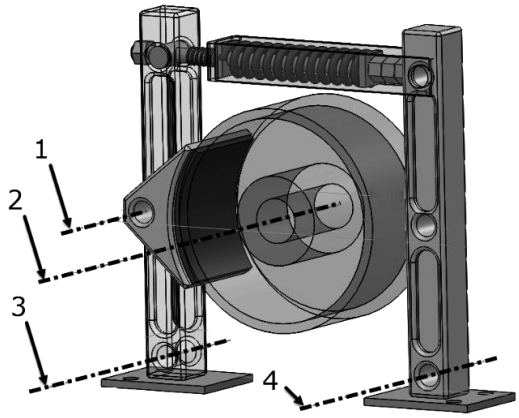

Fig. 5. Parallel primitives in the MBS model of drum brake type TKT-300
(Some of the parts are hidden for the purpose of better visualization)
1 – axis of rotation of the shoe, 2 – axis of rotation of the drum,
3, 4 – axes of rotation of the levers

The addition of the two parallel primitives causes two redundant constraints, due to the two rotating joints defined at each of the axes of rotation of the shoes around the levers.

To obtain zero redundant constraints in the MBS model of the TKT-300 brake type, the bushings approach is applied, i.e., elastic bushings are added to the redundant joints. These bushings play the role of elastic connections, which have a corresponding translational and rotational stiffness and damping.

In this case, two bushings are added, one at each of the axes of rotation of the respective shoe 2 around the lever 1, Fig. 3. Bushings are assumed to be made of steel, from which the corresponding translational stiffness of the bushings is determined. Damping, as well as the rotational stiffness are neglected.

From the check, Table 2, as well as from the model motion tests, it is established that the motion of the model corresponds to the motion of the actual assembly. Also,

there are no redundant constraints that would lead to the occurrence of unrealistic forces and moments.

Similarly, the SIME 45K disc brake model has also been developed.

In the present studies, it is perceived that the drum/disc has reached its steady angular velocity and then the brake is actuated. In this case, the drum/disc is brought in motion by an appropriate value of initial angular velocity. The gravity is taken into account, as well as the friction in the bearings on which the drum/disc rests.

The brake type TKT-300 is actuated by the spring 5, Fig. 3.

The spring in the MBS model, both of the TKT-300 brake and of the SIME 45K brake, is represented by a simulation element – linear spring element, Fig. 6 – position 1, where appropriate stiffness k_s and damping can be set. In this case, the damping of the simulation element is neglected.

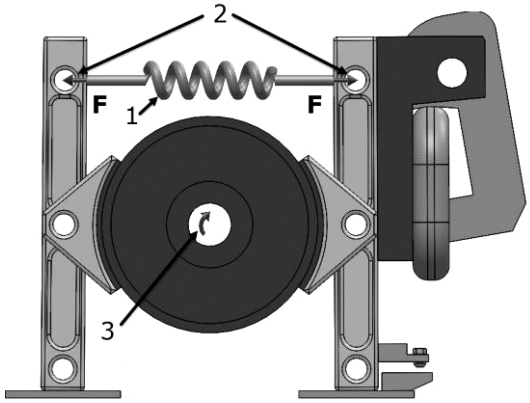

Fig. 6. Simulation elements in the MBS model of drum brake type TKT-300
(Some of the parts are hidden for the purpose of better visualization)
1 – spring element, 2 – balancing forces F, 3 – force element (torque)

The stiffness k_s is calculated from the known relation $k_s = F_s/f$.

The force F_s is calculated according to the type of the brake for preset geometric, kinematic and power parameters.

The spring force, created during braking, develops instantly. This force must develop for a specific time period, corresponding to about 0.1s, which is, for example, the time required to rotate the armature 6, Fig. 3 after power failure. To achieve this effect in the MBS model, forces $F = F_s/2$ (Fig. 6 – position 2) that balance the spring force, are applied at the points on the levers 1, where the spring force acts.

Each of the two balancing forces F is a smooth step forcing function, defined in the local coordinate system. When building the function, the following expression is used [22]:

$$STEP(t, F_1, t_1, F_2, t_2). \tag{14}$$

This function is a built-in function in SolidWorks Motion, where the designations are: t is the time to develop the function, the pairs (t_1, F_1) and (t_2, F_2) represent the corresponding values of the force at the times t_1 and t_2. The *STEP* function is a cubic interpolation of the Heaviside's step function

$$F(t) = \sum_{i=0}^{n} F_i \chi_{A_i}(t), \tag{15}$$

where n is the number of intervals, A_i is the corresponding interval, F_i is the value of the force in the interval A_i, χ_A is indicator function of A

$$\chi_A(t) = \begin{cases} 1, & t \in A, \\ 0, & t \notin A. \end{cases} \tag{16}$$

An essential aspect of the MBS modeling is the construction of the contact. Here, the impact-function-based algorithm [22, 23] is applied successfully to model the contact between the shoes/pads and the drum/disc. Using this algorithm, the contact force is calculated by the equation

$$F_n = kp^n + STEP(a, x_1, y_1, x_2, y_2)\frac{\mathrm{d}p}{\mathrm{d}t}, \tag{17}$$

where k is a stiffness coefficient, n – exponent.

The function $STEP(a, x_1, y_1, x_2, y_2)$ is represented as

$$STEP(a, x_1, y_1, x_2, y_2) = \begin{cases} y_1, & a \leqslant x_1, \\ y_1 + (x_2 - x_1)z^2(3 - 2z), & x_1 < a < x_2, \\ y_2, & a \geqslant x_2, \end{cases} \tag{18}$$

where $z = \dfrac{a - x_1}{x_2 - x_1}$.

For the present case $x_1 = y_1 = 0$, $a = p$, $x_2 = p_{\max}$, $y_2 = d_{\max}$, where $p_{\max}$ is the max penetration when the max damping $d_{\max}$ is activated.

The algorithm assumes that the contact force consists of two components – stiffness k and damping d.

For all the studied MBS models, the following contact parameters are assumed the same: stiffness $k = 1.1 \times 10^5$ N/mm, damping $d = 1.41$ Ns/mm, max contact penetration $p_{\max} = 0.1$ mm, exponent $n = 1.5$.

The balancing force functions are designed so as to allow simulations to be carried out on different brake designs – brakes with a short-stroke electromagnet or brakes with a hydraulic thruster.

The reaction torque $\pm T_R$ can be with either a (+) or a (−) sign, which is accounted for in the MBS models by the use of a corresponding force element,

position 3, Fig. 6 from the SolidWorks Motion library. For this case, the value of the force element is determined by the equation [2]:

$$T_R = \frac{QD\beta}{2u_M}, \tag{19}$$

where D is the diameter of the drum on which the rope is wound, when lifting $\beta = 1/\eta_M$, when lowering $\beta = \eta_M$, assumed $\eta_M = 0.8$, according to [2].

The direction of action of the force element may either coincide with the direction of the nominal angular velocity ω of the drum/disc rotation, or be in the opposite direction, depending on the case under consideration.

3.4. Preparation of the MBS models for simulation studies

This is the final stage of the MBS model preparation before proceeding to adequacy checks, simulation studies, reporting of results and building databases of simulation results. Considerable attention in this stage is devoted to the selection of the proper integrator type. SolidWorks Motion offers three possible types of integrators to solve the problem: GSTIFF, WSTIFF and SI2_GSTIFF.

For the present study, in which impacts are inevitable during the braking process (contacting of the friction lining with the drum/disc), it is essential that the simulation be stable and that accurate results are obtained with significantly reduced time steps for the solution. Therefore, attention is directed to the use of the SI2_GSTIFF integrator.

SI2_GSTIFF is essentially the same integrator as GSTIFF but with added SI2 stabilization method. In this way, the SI2_GSTIFF solves accurately for the speeds and accelerations, is very stable with small time steps and is able to accurately monitor the high frequency fluctuations (for example, the impacts at the moment when the brake is applied). The problem with this method is in the increased computational time, and also if the model has input velocity as a function of time, this function must be continuous or differentiable.

In the current case, the constructed model applies the steady drum angular velocity as the initial condition and at a later point in time the brake is applied. This avoids the solution problems related to the integrator and the input velocity as a function of time as described above.

4. Simulation studies

4.1. Adequacy of the 3-D models

The constructed computer models, as described above, have been used for numerous multibody transient local computer 3-D simulations. This article includes the results of the following four simulation cases:

Case 1 – external, linearly acting, centrally pivoted shoe drum brake, experimentally tested in [1],

Case 1u – external, linearly acting, centrally pivoted shoe drum brake, used for the calculations in [2],

Case 2 – this is Case1 retrofitted with caliper disc brake,

Case 2u – this is Case1u retrofitted with caliper disc brake.

In this connection, the used subscripts of 1, 1u, 2 and 2u of the corresponding quantities indicate that the corresponding quantity belongs to the studied case, unless otherwise mentioned.

The adequacy of the computer models is confirmed by comparing the results of simulations, performed with the models, with the results of computational models [2] and [18], and a field test on a stand [1].

In [2] a TKT-300 type brake has been selected as an element in the kinematic chain of a bridge crane hoisting mechanism and calculations have been done with the following data: $Q = 12.5$ ton, $J_{1u} = 1.245$ kgm^2, $T_B = 373.14$ Nm (for medium duty cycle and load speed $v = 0.15$ m/s), $T_R = 213.2$ Nm, $\omega = 73.3$ s$^{-1} \approx 700$ rpm, $R_d = 150$ mm (at $\omega \approx 700$ rpm, the peripheral speed of the drum is $v_p = 11$ m/s), friction material – asbestos strip with coefficient of friction $\mu = 0.33$.

The following have been calculated: $t_{Bu1} = 0.156$ s, $t_{Bu2} = 0.571$ s and the normal force $F_N = 3775.56$ N with which the shoe acts on the drum.

A comparative analysis has been carried out between the computational model in [2] and the constructed 3-D model of the selected brake for the following input parameters of the model $J_{1u} = 1.245$ kgm^2, $T_R = 213.2$ Nm, $\omega = 73.3$ s^{-1}, $\mu = 0.33$, $\lambda = 0.75$ mm.

The comparative analysis is given in Table 3.

Table 3.

Brake type TKT-300 comparative analysis

Parameter	Model		
	Computational model	3-D model	Error Δ [%]
t_B [s]	0.156	0.152	2.36
T_B [Nm]	373.14	372.64	0.13
F_N [N]	3775.56	3764.03	0.31

Note: F_N is the normal force on a single shoe

A field experiment on a stand has been done in [1], using a TKT-300 type brake with the following parameters: $T_B = 490.33$ Nm, $\mu = 0.42$, average circumferential drum speed $v_p \approx 11$ m/s ($\omega = 73.3$ s^{-1}), $J_1 = 11.166$ kgm^2 and assumed $T_R = 0$.

Fig. 1 shows the braking time $t_B = 1.67$ s and the variation of the braking torque during the braking process. Fig. 7 shows the braking time t_B and the variation of the braking torque T_B as results of a simulation with the 3-D model of the brake type TKT-300.

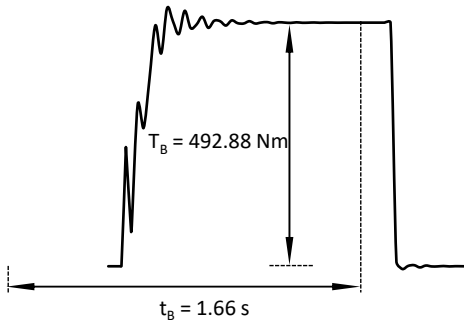

Fig. 7. Variation of the braking torque of the 3-D computer MBS model of brake type TKT-300

The input parameters of the 3-D model are: $J_1 = 11.166$ kgm^2, $T_R = 0$, $\omega = 73.3$ s^{-1}, $\lambda = 0.75$ mm, $\mu = 0.42$.

Table 4 shows the comparative analysis between the experiment given in [1] and the 3-D model of the brake.

Table 4.

Brake type TKT-300 comparative analysis

Parameter	Model		
	Experiment	3-D model	Error Δ [%]
t_B [s]	1.67	1.66	0.6
T_B [Nm]	490.33	492.88	0.52

For the disc brake type SIME 45K, a comparative analysis has been performed between the algorithm based computational model given in [18] and the results of a computer simulation with the constructed 3-D computer model. The input parameters of the computational model are: $T_B = 490.33$ Nm, $J_2 = 10.9$ kgm^2, $T_R = 0$, $\omega = 73.3$ s^{-1}, wrap angle of the friction element 60°, friction radii, Fig. 2, $R_o = 155$ mm, $R_i = 115$ mm, $k_f = 1.01$, $\mu = 0.42$. The input parameters of the 3-D model are: $J_2 = 10.9$ kgm^2, $T_R = 0$, $\omega = 73.3$ s^{-1}, $\lambda = 0.3$ mm, $\mu = 0.42$.

The obtained results used for the comparative analysis are given in Table 5.

Table 5.

Brake type SIME 45K comparative analysis

Parameter	Model		
	Computational model	3-D model	Error Δ [%]
t_B [s]	1.63	1.64	0.6
F_N^* [N]	4323.92	4335.6	0.27
F_B^{**} [N]	1816.05	1820.96	0.27

$^*F_N$ is the normal force on a single pad;
$^{**}F_B$ is the braking force on a single pad

From the comparative analysis it is clear that the constructed computer models are adequate approximations of the actual brakes.

4.2. Results and analyses

The simulation studies of both types of brakes (drum and disc brakes) have been performed for the following ranges:

- gap between the friction lining and the disc/drum $\lambda = 0.3 \div 1.3$ mm;
- time for increasing the braking force 0.1÷0.4 s;
- coefficient of friction $\mu = 0.33 \div 0.5$;
- spring stiffness $k_s = 40$ N/mm (the value is assumed the same for all models).

Some of the obtained results are given in the graphs below.

Fig. 8 shows the results of the TKT-300 brake simulation test, with model input parameters: $J_1 = 11.166$ kgm^2, $T_R = 0$, $\omega = 73.3$ s^{-1}, $\lambda = 0.75$ mm, $\mu = 0.42$.

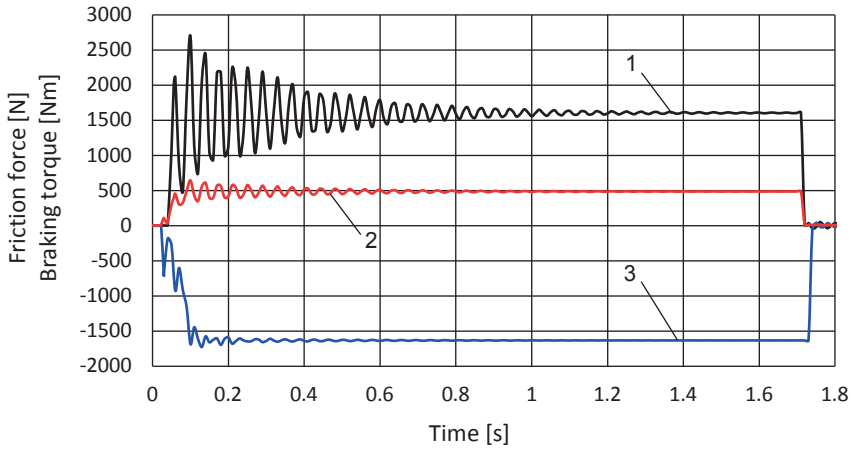

Fig. 8. Results of the TKT-300 brake simulation test 1 – friction force [N] at the lever carrying the electromagnet, 2 – braking torque [Nm], 3 – friction force [N] at the lever not carrying the electromagnet

From the results presented, it can be seen that there is a great difference in the dynamics of the friction forces at the two levers carrying the shoes. The friction force dynamics at the lever carrying the electromagnet (dynamic coefficient 1.67) is considerably greater than the dynamics of the friction force at the lever that does not carry the electromagnet (dynamic coefficient 1.06). This difference in the dynamic response of the two friction forces is due to the difference in the moments of inertia of the two levers by which the shoe-drum contact is realized.

The lever, to which the MO-300B electromagnet with mass of 40 kg [20] is attached, has a considerably greater moment of inertia than the lever that carries only the brake shoe.

In connection with this, after the brake is actuated, the two shoes do not come simultaneously in contact with the drum, which results in unbalanced contacting of the friction pairs. As a result, a short-term impact loading occurs.

From simulation tests of the same brake type TKT-300, with a gap between the brake drum and the shoes of 0.6, 0.75, 1 and 1.3 mm, for the case of braking during load descent ($T_R = -213.2$ Nm) a dynamic coefficient K_d has been estimated as a function of the gap, Fig. 9. The dynamic coefficient is calculated as the ratio of the maximum dynamic friction force to the static friction force.

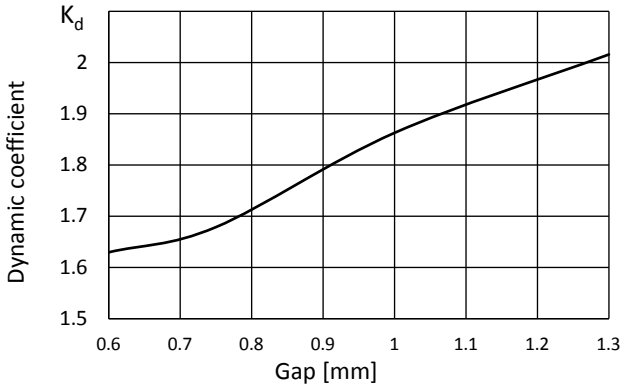

Fig. 9. Variation of the dynamic coefficient obtained from simulations with the 3-D model of the brake type TKT-300

The simulation of the gap between the brake drum and the shoes is accomplished by the use of Hinge mates located along the axes 3 and 4, Fig. 5. These mates set a pre-rotated position of the levers so that the shoes, fastened to the levers do not contact the brake drum at the initial moment but be spaced to a distance equal to the pre-defined gap.

For the studied case, the drum has been assumed as perfectly round.

The results of this study show that the braking dynamics significantly increases with the increase of the gap between the brake drum and the shoes. For gaps greater than 0.6 mm, the braking dynamics increases rapidly. For a gap of 1.2 mm to 1.3 mm, the dynamic coefficient reaches a value of $K_d = 2$.

In the case of an eccentrically rotating drum or in the case of rotating an out of roundness drum, the friction lining on the shoes cannot properly contact with the drum. This creates an uneven braking force and leads to rapid or uneven wear of the friction material, which may cause vibrations or locking of the brake.

A TKT-300 brake simulation study has been conducted, that accounts for an allowable eccentricity, as well as for an out of roundness of 0.25 mm [24], which is applied to simulate the case of radial run-out and an oval brake drum.

The input parameters of the model are: $J_u = 1.245$ kgm^2, $T_R = 213.2$ Nm, $\omega = 73.3$ s^{-1}, $\lambda = 0.3$ mm, $\mu = 0.33$.

The simulation of radial run-out has been accomplished through a motion study mate of type Hinge, which has been suitably constructed and located at the brake drum hub.

The concentricity or radial run-out of this mate is between the axis of the brake drum and the axis of the shaft carrying this drum.

A procedure has been performed to determine the radial displacement of the brake drum axis in the mate. The procedure consists of the following steps.

Step 1 Two mutually perpendicular planes are constructed in the drum-shaft subassembly. The planes pass through the shaft axis and cross the brake drum. One of the planes is assumed to be fixed (in this case, it is the horizontal plane) and the other plane (the vertical) can be translated along the fixed plane, to a certain distance from the axis of the shaft, in one or the reverse direction.

Step 2 After translating the vertical plane at a distance of 0.25 mm, the intersection axis of the two planes is found. This intersection axis is the radially displaced axis of the brake drum.

Step 3 The brake drum is rotated around the radially displaced axis, resulting in the simulation of the radial run-out case.

The simulation of the oval brake drum is based on the assumption of an elliptical shape model of the drum. The ellipse, by the help of which the model is constructed, has the maximum diameter of the drum for its major axis, and the nominal diameter of the drum for its minor axis. The major axis value is obtained from the nominal diameter plus the doubled value of the ovality. For a nominal brake drum diameter of 300 mm and ovality of 0.25 mm, the maximum diameter is 300.5 mm. With these values of the two axes, an ellipse is sketched, which is then extruded to form the oval model of the brake drum.

Fig. 10 shows the variation of the friction moment with and without radial run-out. Fig. 11 shows the dynamic response of the friction moment for the cases of a round drum and an oval drum.

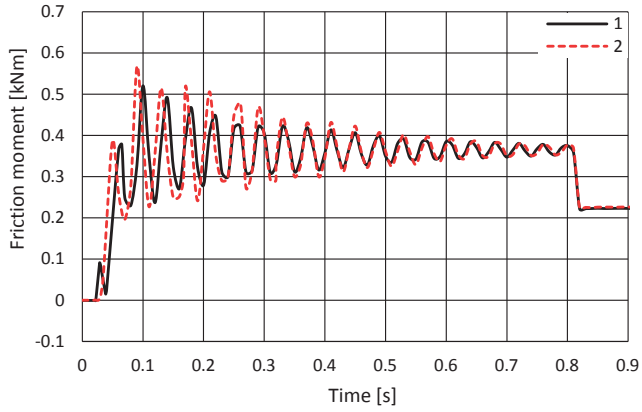

Fig. 10. Variation of the friction moment obtained in a simulation with the 3-D model of the brake type TKT-300 1 – no radial run-out, 2 – with radial run-out of 0.25 mm

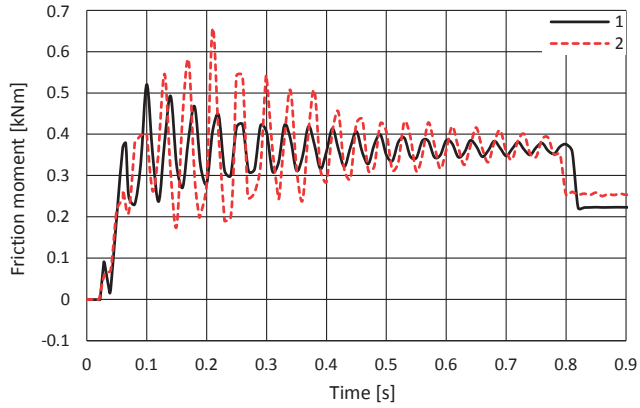

Fig. 11. Variation of the friction moment obtained in a simulation with the 3-D model of the brake type TKT-300 1 – round drum, 2 – drum with ovality of 0.25 mm

It is evident from the obtained results, as shown in Fig. 10 and Fig. 11, that the braking dynamics increases significantly in the presence of radial run-out (coefficient of dynamics 2.48), as well as in the presence of ovality (coefficient of dynamics 2.64).

The sensitivity of the disc brake to radial run-out is almost insignificant compared to the sensitivity of the drum brake. Simulations with SIME 45K confirm this.

A comparative analysis of the dynamic response of brake type TKT-300 and brake type SIME 45K has been done.

The input parameters of the models are as follows:

- for brake type TKT-300 $J_1 = 11.166$ kgm^2 and $J_{1u} = 1.245$ kgm^2;
- for brake type SIME 45K $J_2 = 10.9$ kgm^2 and $J_{2u} = 0.987$ kgm^2 (the values are estimated from Eq. (11), where $J_{drum} = 0.378$ kgm^2 and $J_{disc} = 0.12$ kgm^2 are taken from Table 1), $\omega = 73.3$ s^{-1} and $\lambda = 0.3$ mm are the same for all models.

Fig. 12 shows results of the performed comparative analysis.

The following dynamic coefficients have been reported:

- for case 1, the dynamic coefficient is 1.19,
- for case 2, the dynamic coefficient is 1.05,
- for case 3, the dynamic coefficient is 1.34,
- for case 4, the dynamic coefficient is 1.08.

The results of several simulation cases of braking with brake type TKT-300 and brake type SIME 45K have been compared: case 1 vs. case 2 at $T_R = 0$, case 3 vs. 4 for braking during load lift at $T_R = 213.2$ Nm.

It has been recognized from the comparative analysis that the dynamic response of the SIME 45K brake (cases 2 and 4) compared to the TKT-300 response (cases 1 and 3) is significantly lower, although the input parameters are almost the same. This is explained by the difference in the design of the two brakes. With SIME 45K, one of the vertical levers (pillars) is fixed and the other lever is movable. The fixed

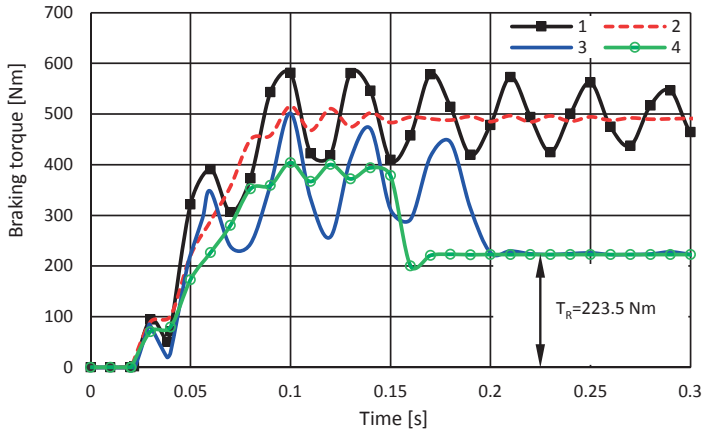

Fig. 12. Variation of the braking torque For TKT-300 (1 – for J_1 and $\mu_1 = 0.42$, 3 – for J_{1u} and $\mu_u = 0.33$) For SIME 45K (2 – for J_2 and $\mu_2 = 0.42$, 4 – for J_{2u} and $\mu_u = 0.33$

lever carries the electromagnet of the brake. The movable lever, which is suitably connected to the armature of the electromagnet, is driven by a one-sided compressed spring, one end of which is connected to the fixed lever and the other end is connected to the anchor of the electromagnet. When the electric power supply is cut off, the spring is released and the anchor moves together with the movable vertical lever. Along with the movable vertical lever, a horizontal lever-cam mechanism is also driven. In this way, the brake pads are simultaneously contacting the brake disc. The design of the brake is dynamically balanced, resulting in a significant reduction in the dynamics when switching on and off of the electromagnet.

In the case of the disc brake, depending on the design, a dynamic loading is generated that loads the shaft. In this connection, using the SIME 45K 3-D brake model, simulation studies for the arrangements shown in Fig. 13 have been performed.

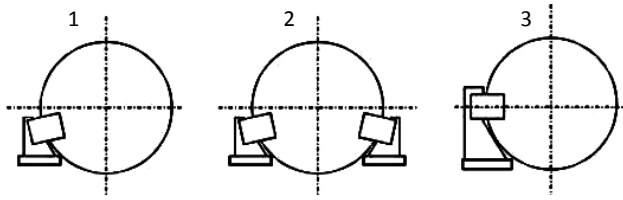

Fig. 13. Disc brake arrangements

The input parameters of the model are: $J_2 = 10.9$ kgm^2, $T_R = 0$, $\omega = 73.3$ s^{-1}, $\lambda = 0.3$ mm, $\mu = 0.42$.

The results for the dynamic force that loads the shaft are given in Fig. 14. The labels in Fig. 14 correspond to the arrangements shown in Fig. 13.

For cases 1 and 2, the manufacturer recommends an angle of 17° inclination of the calipers to the horizon. An experiment, marked 2* at an angle of 30° of the

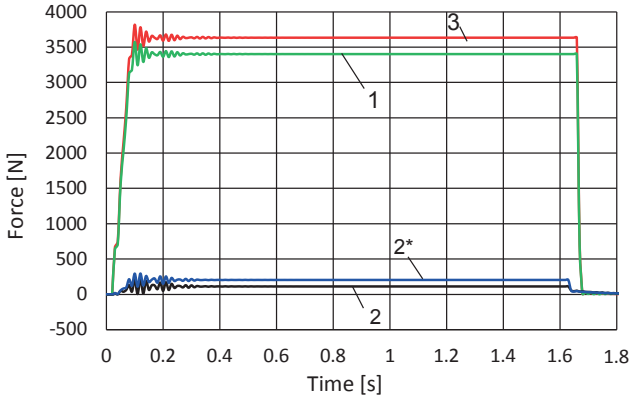

Fig. 14. Variation of the dynamic force that loads the shaft during braking (the mass of the brake disc is not taken into account

calipers, has also been performed. It is found that in cases 1 and 3, after the brake is applied, the shaft is significantly loaded during braking. For case 1, the dynamic force value is 3401 N, and for case 3 the value of the dynamic force is 3634 N.

In case 2, the dynamic force value is 112 N, and in case $2^{\star}$ the dynamic force value is 203 N.

From the results, presented in Fig. 14, it has been found that in design cases 1 and 3 of the studied disc brake, a significant dynamic force is produced that loads the shaft. For unloading of the shaft, the most suitable case is case 2, in which the pads are placed at an angle of 17° to the horizon.

The constructed drum brake MBS models allow one to do research on the performance of hydraulically-driven brakes.

Simulations of the operation of brake type TKTG-300M have been performed. The parameters are similar to those of the TKT-300 brake. The nominal torque of the TKTG-300M brake is 80 kgfm, but for the purposes of the present study it is adjusted to 50 kgfm. The brake is triggered by means of a TGM-50 hydraulic thruster with piston descending time of 0.37 s.

The input parameters of the simulation model are: $J_u = 1.245$ kgm^2, $T_R = 213.2$ Nm, $\omega = 73.3$ s^{-1}, $\lambda = 0.75$ mm, $\mu = 0.33$.

Fig. 15 shows the dynamics of the brake forces for brake TKTG-300M and brake TKT-300. The simulation test has not taken into account the mass of the electromagnet and the mass of the hydraulic thruster.

The results of the comparative simulation study between the dynamics of the friction force (acting on a single shoe) of a hydraulically-driven drum brake and an electromagnet-driven drum brake, show that the braking dynamics improves significantly when using the hydraulic thruster. This is largely explained by the increased braking time, which, for the tested brake TKTG-300M, is about 67% greater than the braking time of the TKT-300 brake.

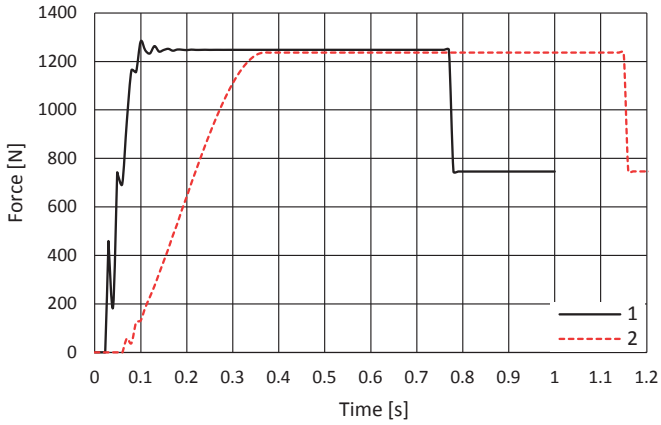

Fig. 15. Variation of the friction force that acts on a single shoe
1 – TKT-300, 2 – TKTG-300M

5. Conclusions

By creating adequate computer 3-D MBS models of real brakes, simulation research and analyses have been performed on aspects of the dynamics of drum and disc brakes, when the brakes are used in the hoisting mechanisms of cranes.

A significant influence on the dynamics of the studied friction braking systems has the following: the brake design, deviations from the roundness/flatness of the working surface of the rotating brake element, deviations in the kinematic chain when mounting the rotating brake element on the shaft (deviations from concentricity), the gap between the friction braking elements; the type and mode of brake drive.

In drum brakes with automatic (electromagnetic) drive, where the electromagnet is suspended to one of the two movable levers, due to unbalanced contact in the friction pairs, a significant short-term dynamic load develops. When increasing the gap between the brake drum and the shoes, the dynamics increases considerably – for a gap of 1.2 mm to 1.3 mm, the dynamic coefficient reaches $K_d = 2$, assuming a perfectly round drum.

The presence of radial run-out or ovality has a significant impact on the dynamics of drum brakes. For a gap of $\lambda = 0.30$ mm, between the drum and the shoes and equal values of 0.25 mm for the ovality and radial run-out, there are high dynamic loads observed and the dynamic coefficient reaches 2.64, in the case of ovality, and 2.48 in the case of radial run-out.

The dynamic response of the disk brake is considerably smaller than the dynamic response of the drum brake. This is due to the simultaneous contact of the pads with the brake disc, which is accomplished by a proper dynamically balanced brake design.

The sensitivity of the disc brake to radial run-out (eccentric disc) is almost negligible to that of the drum brake.

In the case of disc brakes with one pair of pads, a significant dynamic force is generated, that loads the shaft. Two or more friction pairs are used to reduce the magnitude of this force. Simulation studies in this direction show that the smallest radial force value is obtained by placing the pads at an angle of 17° to the horizon, which confirms the manufacturer's recommendation.

The use of hydraulic thruster in drum and disc brakes leads to a significant reduction in dynamic impacts but significantly increases the braking time.

Manuscript received by Editorial Board, February 28, 2018;
final version, May 22, 2018.

References

[1] M.P. Alexandrov. *Brakes for material handling machines*. Moscow, 1976. (in Russian)
[2] F.K. Ivanchenko. *Calculations of material handling machines*. Kiev, 1978. (in Russian)
[3] *Ican Company Ltd*. www.ican.co.jp/en.
[4] R. Limpert. *Brake Design and Safety*. 3rd edition, SAE International, 2011.
[5] D. Keyser. *Selection Procedures for Brakes*. MICO Incorp., 1992.
[6] A. Belhocine, A.R. Abu Bakar, and M. Bouchetara. Numerical Modeling of disc brake system in frictional contact. *Tribology in Industry*, 36(1):49–66, 2014.
[7] A. Belhocine and M. Bouchetara. Structural and thermal analysis of automotive disc brake rotor. *Archive of Mechanical Engineering*, 61(1):89–113, 2014. doi: 10.2478/meceng-2014-0005.
[8] A. Belhocine, A.R. Abu Bakar, and O.I. Abdullah. Structural and contact analysis of disc brake assembly during single stop raking event. *Transactions of the Indian Institute of Metals*, 68(3):403–410, 2015. doi: 10.1007/s12666-014-0468-6.
[9] M.R. Ishak, A.R. Abu Bakar, A. Belhocine, J.M. Taib, and W.Z.W. Omar. Brake torque analysis of fully mechanical parking brake system: Theoretical and experimental approach. *Measurement*, 94:487–497, 2016. doi: 10.1016/j.measurement.2016.08.026.
[10] A. Belhocine and N.M. Ghazaly. Effects of Young's modulus on disc brake squeal using Finite Element Analysis. *International Journal of Acoustics and Vibration*, 21(3):292–300, 2016. doi: 10.20855/ijav.2016.21.3423.
[11] A. Belhocine and W.Z.W Omar. Three-dimensional finite element modeling and analysis of the mechanical behavior of dry contact slipping between the disc and the brake pads. *The International Journal of Advanced Manufacturing Technology*, 88(1–4):1035–1051, 2017. doi: 10.1007/s00170-016-8822-y.
[12] A. Belhocine. FE prediction of thermal performance and stresses in an automotive disc brake system. *International Journal of Advanced Manufacturing Technology*, 89(9–12):3563–3578, 2017. doi: 10.1007/s00170-016-9357-y.
[13] A. Belhocine and W.Z.W. Omar. CFD analysis of the brake disc and the wheel house through air flow: Predictions of Surface heat transfer coefficients (STHC) during braking operation. *Journal of Mechanical Science and Technology*, 32(1):481-490, 2018. doi: 10.1007/s12206-017-1249-z.
[14] J-S. Li and Y. Liu. Study on the rigid-flexible couple of drum brake system. 7th International Conference on Computer Science & Education (ICCSE&), 14–17 July 2012, Melbourne, Australia. doi: 10.1109/ICCSE.2012.6295112.
[15] F. Talati and S. Jalalifar. Analysis of heat conduction in a disk brake system. *Heat and Mass Transfer*, 45:1047-1059, 2009. doi: 10.1007/s00231-009-0476-y.

[16] D. Lie and C.K. Sung. Synchronous brake analysis for a bicycle. *Mechanism and Machine Theory*, 45(4):543–554, 2009. doi: 10.1016/j.mechmachtheory.2009.11.006.
[17] R.S. Kajabe and R.R. Navthar. Optimization of Disc Brake Rotor with Modified Shape. *International Journal of Research in Aeronautical and Mechanical Engineering*, 3(3):52–60, 2015.
[18] R.G. von Budynas, J.K. Nisbett. *Shigley's Mechanical Engineering Design*, 8th edition, McGraw-Hill, 2008.
[19] A. Shabana. *Dynamics of Multibody Systems*, 4th edition, Cambridge University Press, 2013.
[20] *Company Parametr*. www.9700439.ru/
[21] *Stromag France SIME Brakes*. www.stromagfrance.com/.
[22] *Adams Online Help System*, 2015. www.mscsoftware.com/msc-academic-learning-center.
[23] *SolidWorks Online Help System*, 2015. http://help.solidworks.com.
[24] *Reconditioning brake drums and shoes*, Integrated Publishing, Inc.. www.tpub.com.